

Article

Active Vibration Suppression of a Motor-Driven Piezoelectric Smart Structure Using Adaptive Fuzzy Sliding Mode Control and Repetitive Control

Chi-Ying Lin * and Hong-Wu Jheng

Department of Mechanical Engineering, National Taiwan University of Science and Technology, No. 43, Keelung Rd., Sec. 4, Taipei 106, Taiwan; kingiffe@gmail.com

* Correspondence: chiying@mail.ntust.edu.tw; Tel.: +886-02-2737-6484

Academic Editors: Gangbing Song, Steve C.S. Cai and Hong-Nan Li

Received: 28 December 2016; Accepted: 28 February 2017; Published: 4 March 2017

Abstract: In this paper, we report on the use of piezoelectric sensors and actuators for the active suppression of vibrations associated with the motor-driven rotation of thin flexible plate held vertically. Motor-driven flexible structures are multi-input multi-output systems. The design of active vibration-suppression controllers for these systems is far more challenging than for flexible structures with a fixed end, due to the effects of coupling and nonlinear vibration behavior generated in structures with poor damping. To simplify the design of the controller and achieve satisfactory vibration suppression, we treated the coupling of vibrations caused by the rotary motion of the thin flexible plate as external disturbances and system uncertainties. We employed an adaptive fuzzy sliding mode control algorithm in the design of a single-input-single-output controller for the suppression of vibrations using piezoelectric sensors and actuators. We also used a repetitive control system to reduce periodic vibrations associated with the repetitive motions induced by the motor. Experimental results demonstrate that the hybrid intelligent control approach proposed in this study can suppress complex vibrations caused by modal excitation, coupling effects, and periodic external disturbances.

Keywords: flexible structure; piezoelectric materials; active vibration control; adaptive fuzzy sliding mode control; repetitive control

1. Introduction

Flexible structure based positioning is generally achieved using motors to expand the range of strokes and applications. Examples include the grabbing motion of flexible robot manipulators and the lifting operations of cranes. Due to their poor damping, the coupling of the entire structures, and various nonlinear effects, the rotary motions of flexible structures produce complex vibrations that can severely affect the precision of positioning. A popular and effective research approach to address this issue in recent years has been the use of piezoelectric materials as actuators and sensors in conjunction with active suppression control algorithms to create smart active suppression and control designs for structures [1–3].

Motor-driven flexible structures generally have two control objectives: (1) motor tracking control; and (2) active suppression control of vibrations in flexible structures. Most of these control systems are multi-input-multi-output (MIMO) systems in which achieving the high-performance motion control of these two objectives makes for a certain level of difficulty in controller design. However, discussion regarding these systems usually focuses on vibration-suppression control for the flexible structures. Thus, the majority of existing literature examines the effectiveness of various control methods in active vibration suppression [4–8]. Tso et al. [4] employed proportional-derivative (PD) control to actively

suppress the vibrations in a single-axis flexible robot manipulator. Shan et al. [5] used positive position feedback (PPF) control for the active suppression of vibrations in a flexible robot manipulator with one degree of freedom. Ahmad et al. [6] combined fuzzy control with PD control and input shaping control for the tracking and control of deflection in flexible robot manipulators. Park et al. [7] combined fuzzy controller design with H-infinity control to enhance system robustness in reducing vibrations in a single-axis flexible robot manipulator during positioning. Lin and Chao [8] combined a flexible beam with a beam-cart system to investigate vibration responses during cart motion. They also employed piezoelectric transducers and adaptive neuro-fuzzy control for the active suppression of vibrations in the flexible beam.

Aside from the common single-axis flexible robot manipulators, flexible structures with two or more degrees of freedom enable greater work space and more diverse actions. However, coupling effects and nonlinearities greatly complicate vibration behavior [9–13]. Moudgal et al. [10] took into account the coupling effects between the axes in the design of a fuzzy controller aimed at reducing vibrations in a dual-link flexible robot manipulator. Lin et al. [11] designed a piezoelectric vibration absorber for a beam–cart–seesaw system and suppressed vibration responses in the system by pairing passive mechanical components with active piezoelectric proportional-integral-derivative (PID) feedback control. Lin and Zheng [12] designed a piezoelectric truss structure driven by two motors to enable rotation in two directions. They combined neural-fuzzy control with a genetic algorithm to achieve active vibration suppression control; however, the system was limited to static positioning and did not take into account the vibration responses created by dynamic tracking [13], Lin et al. established a mathematical model to facilitate modal analysis of the large flexible structure in [12]. They also applied a hybrid PD/repetitive control framework [14] for the active suppression of vibrations produced in a thin plate undergoing periodic movement. Their simulation results demonstrated the effectiveness of a hybrid repetitive control (RC) algorithm in suppressing vibration responses in a motor-driven structure. Nonetheless, they treated the entire system and the coupling behavior as linear terms; i.e., they did not take into account the influence of complex coupling terms of the nonlinear terms created by external disturbances in actual flexible structures. Determining whether the same vibration-suppression effects could be obtained in actual rotary systems will require further investigation.

Horizontal thin-plate rotors have been proposed by previous researchers [12,13]. Our primary objective in this study was to determine the effectiveness of an active vibration-suppression control system based on the motor-driven rotation of thin flexible plate held vertically. This system was developed in conjunction with a dynamic model that takes into account nonlinear coupling effects as well as nonlinear terms. We attached piezoelectric devices to the thin flexible plate, which underwent excitation through the periodic motion of the motor. Feedback signals from the piezoelectric sensors were used to examine active vibration-suppression control in the flexible structure. The simulation results in [13] indicate that taking system coupling into consideration during the controller design stage and applying a multi-input-multi-output controller will result in better suppression effects on the vibrations created by periodic disturbances. However, this approach will also greatly increase the complexity of the overall controller design. We sought to overcome these difficulties by assuming that the coupling of vibrations caused by rotary motion could be regarded as external disturbances and systemic uncertainties associated with the thin flexible plate. This led us to design single-input-single-output controllers for the motor-driven rotation system as well as for the piezoelectric vibration suppression system. Adaptive fuzzy sliding mode control (AFSMC) was used in the latter to deal with complex vibrations generated by the rotation of the thin flexible plate. This control method can effectively handle nonlinear systems with uncertain parameters and achieve the expected control performance [15–17]. To minimize the influence of the periodic disturbances caused by the periodic motions of the motor, we adopted a hybrid RC framework [13,14] to combine RC with AFSMC and enhance piezoelectric vibration-suppression control. Experimental results

demonstrate the effectiveness of the proposed hybrid intelligent control method in suppressing the complex vibrations generated in flexible structures subjected to periodic motor-driven rotations.

2. System Modeling

We developed a mathematical model for the large flexible structure used in this study to facilitate subsequent analysis. The structure comprises a large and flexible truss-like thin plate with a servomotor as the driving force. A transmission mechanism enables the rotation of the thin plate around the roll and yaw axes. Piezoelectric actuators and piezoelectric sensors were placed at the root of the vertical thin plate, as shown in Figure 1.

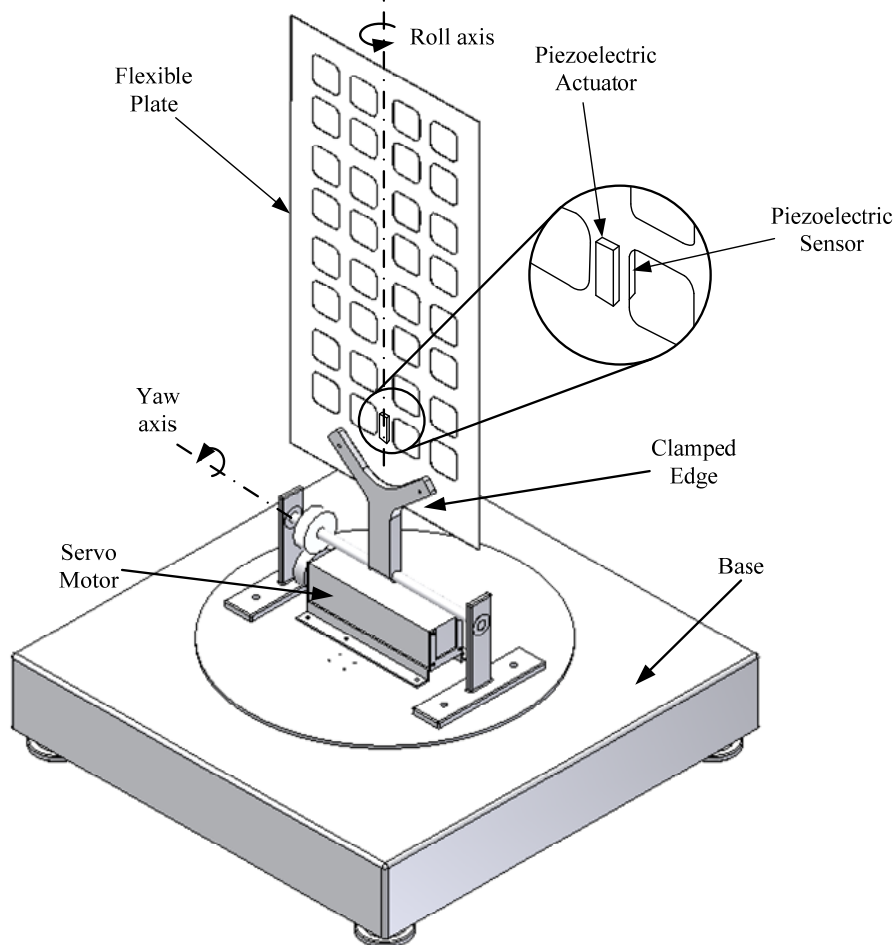


Figure 1. Motor-driven system for the rotation of thin flexible plate held in a vertical position.

In formulating the dynamic equations, we took into account the transverse vibrations in the thin flexible plate. The dynamic equations used for the overall system can be regarded as a combination of the dynamic equations pertaining to a cantilevered thin flexible plate and a servo motor. The thin plate system is treated as linear and the rotation system is assumed to be rigid. The assumptions and derivation procedures used in modeling the overall structure are similar to those in [13]; however, we also included nonlinearities and coupling terms in the current model. When the motor introduces rotary motions, coupling generates disturbances in the thin flexible plate. Vibrations in the thin plate also influence the rotary motions. Based on the effects of coupling, the dynamic equations of the overall system can be written as follows:

$$\mathbf{M}\ddot{\boldsymbol{\eta}} + \mathbf{C}^D\dot{\boldsymbol{\eta}} + \mathbf{K}\boldsymbol{\eta} = \mathbf{B}^P u_p + \boldsymbol{\Phi}_\theta + \mathbf{F} \quad (1)$$

$$\mathbf{L}_a \dot{\mathbf{i}}_a + \mathbf{R}_a \mathbf{i}_a = \mathbf{e}_a - \mathbf{K}_b \dot{\theta}_m \quad (2)$$

$$\mathbf{J}_m \ddot{\theta}_m + \mathbf{B}_m \dot{\theta}_m + \Phi_\eta = \mathbf{K}_i \dot{\mathbf{i}}_a \quad (3)$$

$$\begin{aligned} \mathbf{L}_a &= \begin{bmatrix} L_{ar} & 0 \\ 0 & L_{ay} \end{bmatrix}; & \mathbf{R}_a &= \begin{bmatrix} R_{ar} & 0 \\ 0 & R_{ay} \end{bmatrix}; & \mathbf{e}_a &= \begin{bmatrix} e_{ar} & 0 \\ 0 & e_{ay} \end{bmatrix}; & \mathbf{K}_b &= \begin{bmatrix} K_{br} & 0 \\ 0 & K_{by} \end{bmatrix} \\ \mathbf{J}_m &= \begin{bmatrix} J_{mr} & 0 \\ 0 & J_{my} \end{bmatrix}; & \mathbf{B}_m &= \begin{bmatrix} B_{mr} & 0 \\ 0 & B_{my} \end{bmatrix}; & \mathbf{K}_i &= \begin{bmatrix} K_{ir} & 0 \\ 0 & K_{iy} \end{bmatrix}; & \theta_m &= \begin{bmatrix} \theta_{mr} & 0 \\ 0 & \theta_{my} \end{bmatrix} \end{aligned} \quad (4)$$

where \mathbf{M} and \mathbf{K} denote the mass and stiffness coefficient matrices, respectively; both are $ij \times ij$ diagonal matrices with no coupling between the modes; η is a vector containing modal participation factors with dimensions $ij \times 1$; \mathbf{C}^D is the damping coefficient matrix; \mathbf{B}^P signifies the piezoelectric coefficient matrix; u_p indicates the control input from the piezoelectric actuator; and \mathbf{F} represents the external disturbance. The parameters associated with motor dynamics are as follows. \mathbf{L}_a denotes the inductance constant matrix; \mathbf{R}_a indicates the resistance matrix; \mathbf{i}_a is the current vector; \mathbf{e}_a signifies the motor input voltage vector; \mathbf{K}_b is the back-emf constant matrix; \mathbf{J}_m denotes the inertia matrix; \mathbf{B}_m is the viscous friction coefficient matrix; \mathbf{K}_i is the torque constant matrix; and θ_m denotes the motor angle vector. The subscripts r and y in the above matrices, respectively, refer to servomotor parameters of the roll and yaw axes. Finally, Φ_θ and Φ_η are the coupling function matrices defined as

$$\Phi_\theta = \alpha_c \mathbf{N}^T \mathbf{P}_\theta (\theta, \dot{\theta}, \ddot{\theta}) \quad (5)$$

$$\Phi_\eta = \beta_c \mathbf{N} \mathbf{P}_\eta (\eta, \dot{\eta}, \ddot{\eta}) \quad (6)$$

where \mathbf{P}_θ is a 2×1 nonlinear thin plate displacement function matrix, which originates from motor inertia and friction; \mathbf{P}_η is a $ij \times 1$ nonlinear motor rotation function matrix, in which the influences of the nonlinear terms originate from the flexible vibrations in the lightweight thin plate; α_c and β_c are weighting values in the coupling function; generally, $\alpha_c \gg \beta_c$; and \mathbf{N} is the rigid body coupling matrix defined as

$$\mathbf{N} = \begin{bmatrix} N_r \\ N_y \end{bmatrix} \quad (7)$$

Furthermore, the relationship between the rotation angles of the cantilever thin plate (θ_r and θ_y) and those of the servomotor (θ_{mr} and θ_{my}) can be expressed as

$$\theta = \begin{bmatrix} \theta_r \\ \theta_y \end{bmatrix} = \begin{bmatrix} g_r \theta_{mr} \\ g_y \theta_{my} \end{bmatrix} \quad (8)$$

3. Controller Design for Active Vibration Suppression

In this section, we introduce the control algorithm used in the vibration-suppression control experiments. The AFSMC processes complex vibrations in the thin flexible plate generated in the application of rotary motion. We used a hybrid RC framework [14] incorporating RC to reduce the influence of periodic disturbances created by the periodic motions introduced by the motor.

3.1. Adaptive Fuzzy Sliding Mode Control

The nonlinearity of the mathematical model in the previous section makes it difficult to obtain the relevant state variables. Generally, the format of the fuzzy rule bank in a fuzzy controller is fixed, and the parameters are not updated when the system changes. Consequently, it is difficult to predict control performance in the event of changes to the system parameters. This led researchers to develop AFSMC [15], which combines the advantages of fuzzy control, sliding mode control, and adaptive control. In a control system with unknown parameters, analyzing the input and output data can further understanding of the control system in order to establish language rules. Furthermore, adaptive

control means that the rule bank can be adjusted online, and the robustness can be enhanced via the sliding mode. Figure 2 displays the AFSMC framework, in which gs and gu denote the input and output scaling factors, respectively.

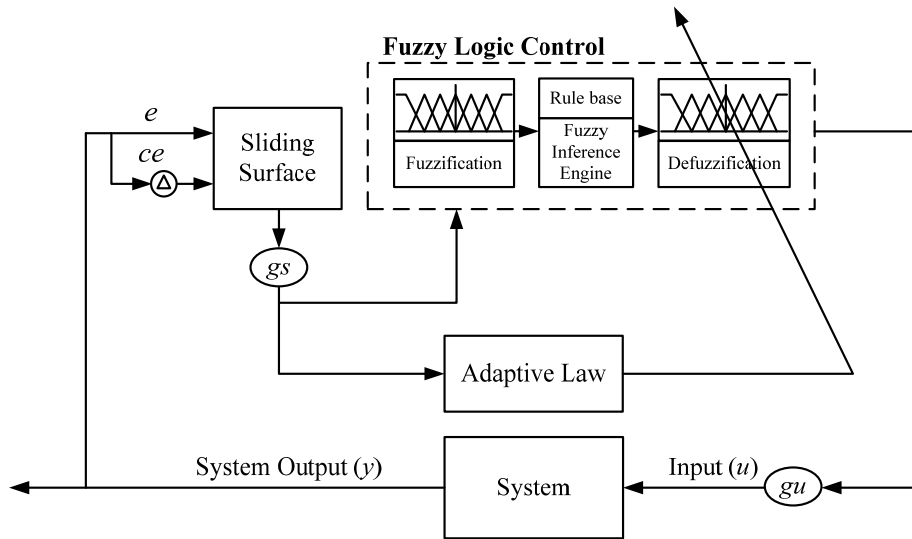


Figure 2. Block diagram of adaptive fuzzy sliding mode control system.

During the design process of the controller, the sliding surface must be defined. In this study, we used a second-order sliding surface, which can be mathematically presented as

$$S(e) = ce + \lambda e \quad (9)$$

where λ is the weight of the sliding mode. Using the sliding surface, we can convert the two-dimensional input variables (e , ce) of the original fuzzy controller into a one-dimensional variable (s). With appropriate scaling based on gs , the input variable can then be input into the fuzzy controller as follows:

$$s(e) = S(e) \times gs \quad (10)$$

As shown in Figure 2, the concept of the controller is to describe physical quantities using linguistic variables and identify the corresponding membership grade. With the adaptive law, the rule table can be adjusted and defuzzified online, which enables the rule bank to begin learning from zero rules. This in turn revises the defuzzified control rules. The control variable can then be obtained using the center of gravity defuzzification method, and then the control input variable is adjusted based on output scaling factor gu .

With regard to fuzzy control, we employed a triangular membership function with seven one-dimensional fuzzy variables for the input variable s and defuzzified variable u , as shown in Figure 3, where NB is the negative big, NM is the negative medium, NS is the negative small, ZO is the zero, PS is the positive small, PM is the positive medium, and PB is the positive big.

In sliding model control, the sliding surface reaching condition is

$$\dot{s} < 0 \quad (11)$$

When $s > 0$, the control variable must be increased to reduce \dot{s} ; if $s < 0$, then the control variable must be decreased to reduce \dot{s} . Input variable s and control variable u can thus be designed to satisfy the reaching condition, where rule i can be written as

$$R_i: \text{IF } s = S_i \text{ THEN } U_i = C_i \quad (12)$$

where S_i is the rule i of the component in question prior to fuzzification; U_i denotes the rule i of the component following defuzzification; and C_i indicates the central position of rule table i of the component following defuzzification. Using the defuzzified U_i corresponding to the i th membership grade obtained from component S before fuzzification, the control variable can be written as

$$u = \frac{\sum_{i=1}^m \mu_i U_i}{\sum_{i=1}^m \mu_i} = \frac{\sum_{i=1}^m \mu_i C_i}{\sum_{i=1}^m \mu_i} \quad (13)$$

where m is the number of rules, with i equaling $1, 2, \dots, m$; the initial values of C_i are all 0, and they are therefore referred to as zero rules. During the control process, we can use the adaptive law to update C_i , the mathematical formula of which is

$$\dot{C}_i(t) = -\gamma \frac{\partial s(t)\dot{s}(t)}{\partial C_i(t)} \quad (14)$$

where γ denotes the adaptive rate. Using the chain rule, we can rewrite Equation (14) into

$$\begin{aligned} \dot{C}_i(t) &= -\gamma \frac{\partial s(t)\dot{s}(t)}{\partial u(t)} \frac{\partial u(t)}{\partial C_i(t)} \\ &= -\gamma c(e)s(t) \frac{\partial u(t)}{\partial C_i(t)} \\ &= \gamma_a s(t) \frac{\partial u(t)}{\sum_{i=1}^m \mu_i(t)} \end{aligned} \quad (15)$$

where $c(e)$ is the direction of the control variable, and γ_a is the learning rate parameter. When errors and error variations exist in the system, C_i increases continually, which causes the system to diverge. To resolve this issue, we can use the adaptive law of e -modification [18] to revise Equation (15) to

$$\dot{C}_i(t) = \gamma_a s(t) \frac{\partial u(t)}{\sum_{i=1}^m \mu_i(t)} - \Lambda |s(t)| C_i(t) \quad (16)$$

where Λ can be adjusted based on system stability, and the learning rate exerts direct impact on the central position of defuzzification. This gives the AFSMC the functions of online learning and updating the defuzzification rule bank. For details on the design process and theory of AFSMC, please refer to [15].

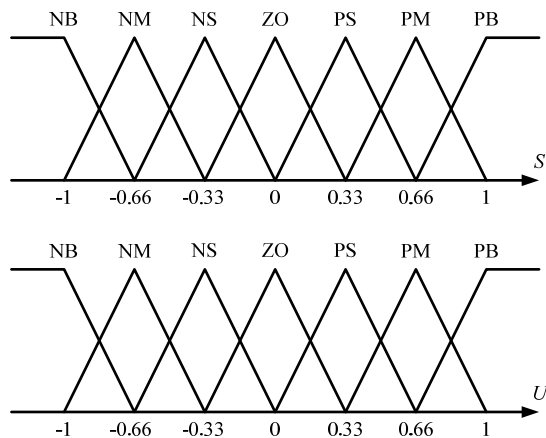


Figure 3. Membership function of AFSMC.

3.2. Hybrid Repetitive Control

Figure 4 presents the hybrid RC framework adopted in this study, where C_1 and C_2 respectively represent the AFSMC controller and the repetitive controller. The sum of the control variable of the repetitive controller, u_{RC} , and the control variable of the AFSMC controller, u_{AFSMC} , is the total control input variable of the system, u_{sum} . In the hybrid control framework used in this study, we designed

the controllers separately with the aim of having them work synergistically. The controller designs are similar to those in [14]; however, we replace PD control with AFSMC control to handle the complex vibration behaviors found in actual flexible structures more effectively.

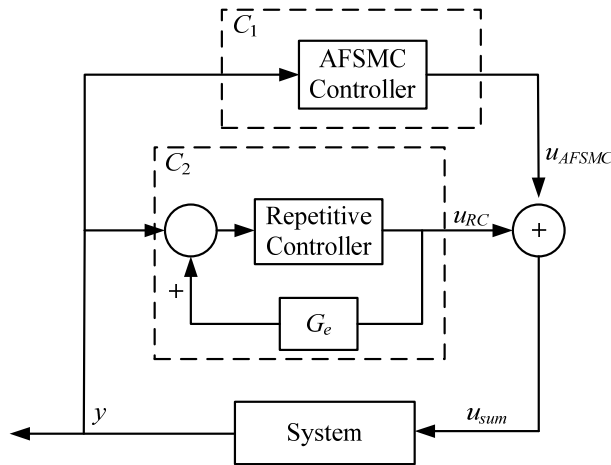


Figure 4. Block diagram of the proposed hybrid AFSMC/RC system.

Periodic disturbances from the external environment or the motions of mechanical structures can damage the system via resonance. Repetitive controllers have proven highly effective in handling periodic signal trajectories and disturbances [19]. Thus, we employed a repetitive controller to eliminate disturbances caused by the periodic motions of the motor. The design principle of a repetitive controller involves adding the internal model of exogenous signals into the feedback control system. According to the internal model principle, asymptotic error tracking can be achieved as long as the closed loop system remains stable [19]. Figure 5 presents a block diagram of the RC adopted in this study.

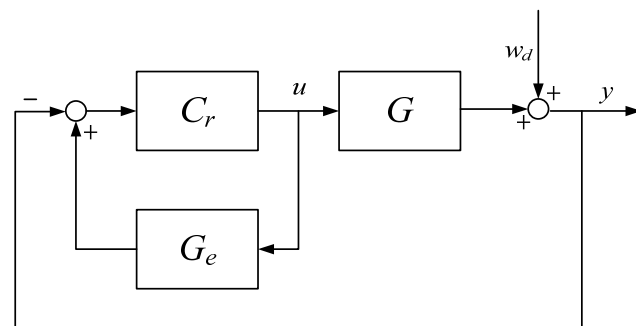


Figure 5. Block diagram of the applied repetitive control system.

In Figure 5, C_r denotes the repetitive controller; G represents the actual system, and G_e symbolizes the mathematical model of the system. As can be seen, the relationship between disturbance w_d and output y in the system of the RC framework is

$$y = \frac{1 - C_r G_e}{1 - C_r (G_e - G)} w_d \quad (17)$$

When the mathematical model G_e approximates the actual system G , Equation (17) can be rewritten as

$$y = (1 - C_r G_e) w_d \quad (18)$$

In this way, the original feedback control issue can be converted into a feedforward control issue. To mitigate the impact of disturbance w_d , a cost function can be established:

$$J_{rc} = 1 - C_r G_e \quad (19)$$

The design objective of this control problem is to derive C_r , the solution to stable plant inversion [20], while satisfying the constraint conditions that accompany periodic signals serving as the exogenous input. For systems with repetitive signals, the internal model D_r can be expressed as $D_r = 1 - z^{-N_d}$ where N_d is the length of the time delay, which is determined by the period of the input signal. If the cost function J_{rc} is written as

$$1 - C_r G_e = R_r D_r \quad or \quad C_r G_e + R_r D_r = 1 \quad (20)$$

then Equation (20) becomes the renowned “Bezout Identity” [21], of which (R_r, C_r) is a solution, and G_e and C_r are coprime. As the piezoelectric vibration suppression system in this study adopts a single-input-single-output control design, the mathematical model of this system, G_e , can be written as

$$G_e = G_d G_i \quad (21)$$

where G_d is the minimal phase of G_e , and G_i denotes the non-minimal phase of G_e .

Substituting Equation (21) into Equation (20) gives

$$\begin{aligned} R_r D_r + C C_i &= 1 \\ C &= C_r G_d \end{aligned} \quad (22)$$

Based on the concept of stable plant inversion in [20], a solution (R_r, C_r) represented in discrete-time can be obtained to fulfill Equation (22):

$$\begin{aligned} R_r &= \frac{1}{1 - (1 - k_r G_i^* G_i) q z^{-N_d}} \\ C &= k_r G_i^* q z^{-N_d} R_r \\ C_r &= C G_d^{-1} \end{aligned} \quad (23)$$

where k_r is the learning gain that can be used to adjust the convergence speed of the repetitive controller, and q is a zero-phase low-pass filter that can enhance the robustness of the repetitive controller. Introducing a narrower bandwidth for filter q results in a repetitive controller of greater robustness but diminishes performance when processing periodic signals, and vice versa. In accordance with Equation (23), the repetitive controller can be expressed as follows:

$$C_r = \frac{k_r G_i^* G_d^{-1} q z^{-N_d}}{1 - (1 - k_r G_i^* G_i) q z^{-N_d}} \quad (24)$$

4. System Setup

The proposed hybrid RC algorithm was implemented in Matlab at a sampling frequency of 1000 Hz for the active suppression of vibrations in a flexible structure. Figures 6 and 7, respectively, present a schematic diagram and photo of the hardware used in the vibration control system. Measurements were obtained using a data acquisition card (NI PCI-6259). After sending control commands to a power amplifier, they were respectively used to drive a servomotor (MHMD-042P1S from Panasonic, Osaka, Japan) and piezoelectric ceramic transducer (SB4020008 from SINOCERAMICS, Shanghai, China). Motor encoder values were sent back to another data acquisition card (MCC PCI QUADO4). Table 1 lists the properties of the thin flexible plate and Table 2 lists the properties of the piezoelectric actuator and piezoelectric thin film sensor used in this study. A piezoelectric amplifier (VP7206 from PiezoMaster, Marlboro, MA, USA) was used to amplify the piezoelectricity from the original piezoelectric actuator by 20 times, thereby generating sufficient bending force to suppress vibrations in the thin flexible plate.

We conducted modal analysis using finite element software to optimize the placement of sensors for subsequent experiments on the suppression of vibration. Due to the large structural mass of the system, we considered only the first bending resonance. In simulations, we applied a 1 Hz sinusoidal moment to the root of the structure and excited the structure for 10 s. We recorded strain values at various locations (A–E in Figure 8) to determine the best location for the sensors used in feedback control. Figures 8 and 9 present the modal analysis associated with various time responses and Fast Fourier transform (FFT) results. The symmetric structure of the device allows us to present strain values on only one side of the thin plate. Our results clearly indicate that vibration was dominated by persistent disturbances with the first vibration mode appearing at approximately 1.5 Hz. Time plots obtained from every location present similar composite periodic responses, whereas the highest strain occurred at the root of the structure (location E), as confirmed by the peak values in the FFT results. We therefore placed the piezoelectric sensor (Model NO. LDT0-028K/L from MEAS, Hampton, VA, USA) at the fixed end of the thin plate, in order to obtain measurements of high sensitivity for use in vibration control. The frequency bandwidth of bandpass filter in the coordinating piezoelectric sensor amplifier (Piezo Film Lab Amplifier from MEAS) was set between 0.1 Hz and 10 Hz. The feedback signals of the piezoelectric vibration suppression system were amplified 10 times.

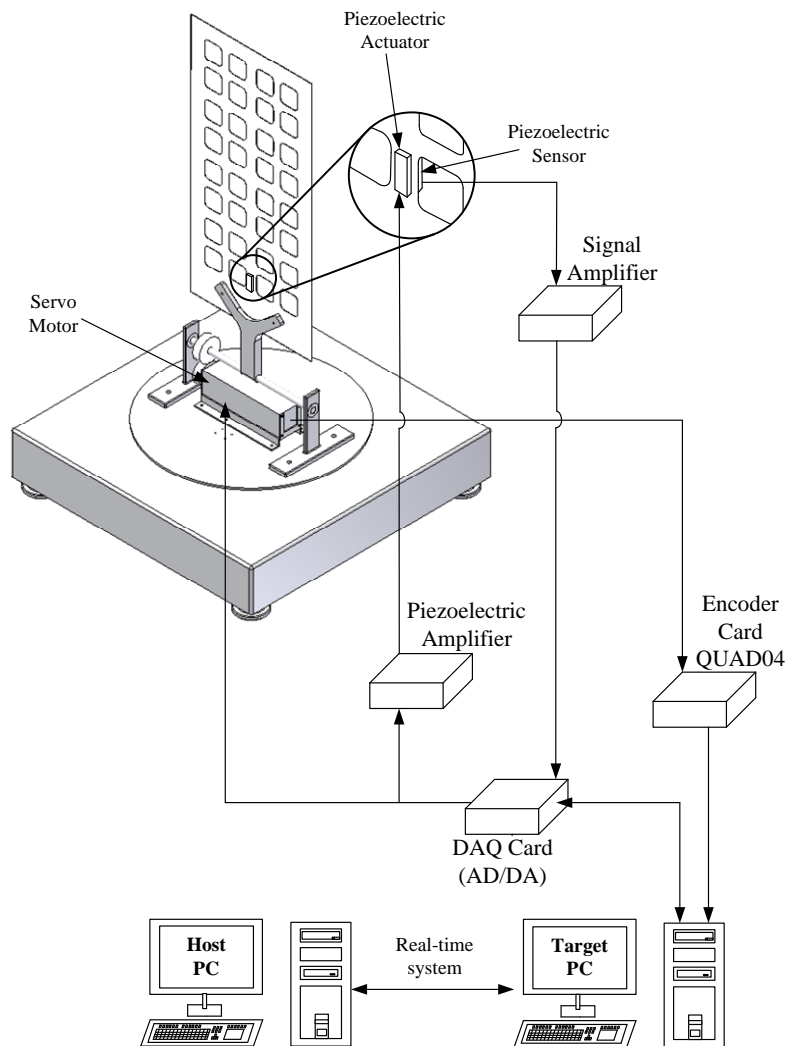


Figure 6. Schematic diagram showing vibration control system for large flexible structures.

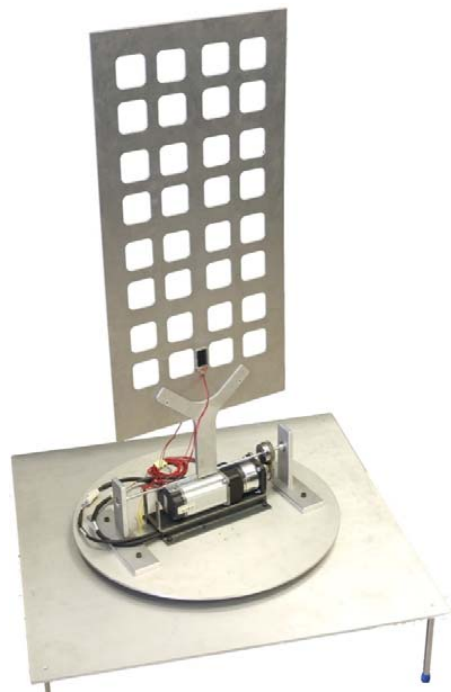


Figure 7. Hardware photograph representing a large flexible structure in experiments.

Table 1. Properties of the flexible plate.

Symbol	Description	Flexible Plate	Units
L_{plate}	Plate Length	700	mm
h_{plate}	Plate Thickness	1.58	mm
W_{plate}	Plate Width	350	mm
ρ_{plate}	Plate Density	2700	Kg/m ³
E_{plate}	Young's Modulus	7.0×10^{10}	N/m ²
ν_{plate}	Poisson Ratio	0.359	N/A

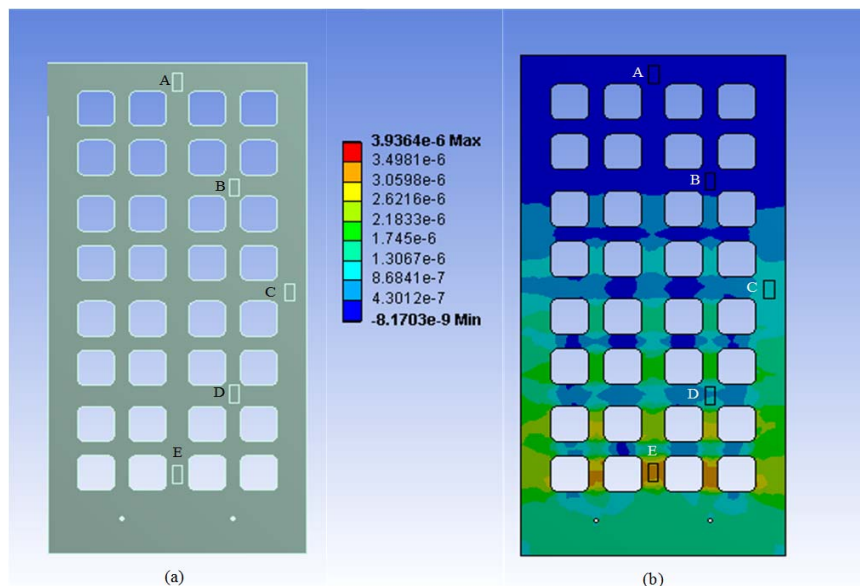
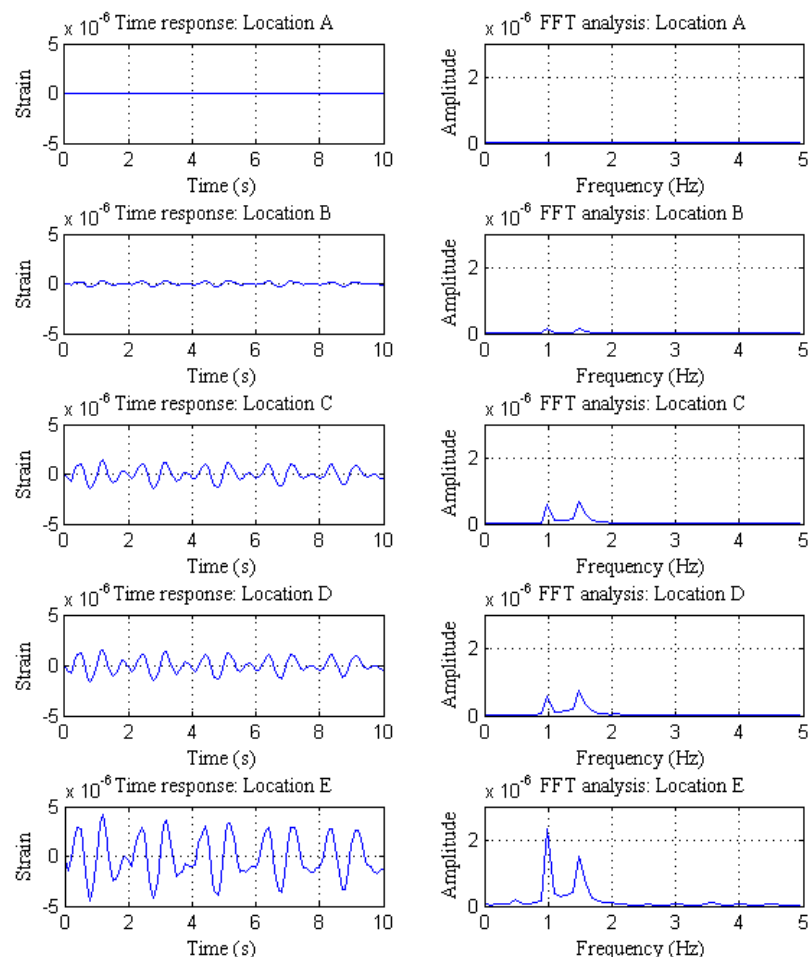


Figure 8. Modal analysis of flexible structure under persistent excitation: (a) illustration of the structure used for modal analysis; and (b) strain distribution throughout entire structure. Capital letters refer to the five locations used in evaluating the placement of piezoelectric sensors.

Table 2. Properties of the applied piezoelectric sensor and actuator.

Symbol	Description	PZT Actuator	PVDF Sensor	Units
L_{px}	Length	40	25	mm
h_p	Thickness	0.8	0.2	mm
L_{py}	Width	20	13	mm
ρ_p	Density	7.4×10^3	1.78×10^3	Kg/m ³
g_{31}	Stress Constant	-8.2×10^{-3}	0.216	Vm/N
d_{31}	Stress Constant	-3.2×10^{-11}	2.3×10^{-11}	C/N
E_a	Young's Modulus	7.1×10^{10}	0.2×10^{10}	N/m ²

**Figure 9.** Modal analysis of flexible structure under persistent excitation. Subplots in the left column show the time responses at each location; subplots in the right column show the corresponding FFT results.

5. Results and Discussion

In the following two sections, we discuss the results of the experiments. In the first section, we discuss the output responses of the motor tracking system without vibration suppression. A proportional-integral (PI) controller was used to track periodic motions introduced by the motor around the yaw axis, and the piezoelectric sensor was used to measure vibrations produced by periodic disturbances in the thin plate. We used this data to identify the primary frequency determining the vibration response, the results of which were verified based on analysis in the frequency domain. We then applied active piezoelectric vibration-suppression control under the same

excitation conditions in order to elucidate the control performance of RC, AFSMC, and the proposed hybrid intelligent control.

5.1. Motor Periodic Excitation

All of the data obtained from piezoelectric sensors passed through an offline fifth-order Butterworth bandpass filter. The frequency range was set at 0.01–50 Hz, and the purpose was to filter out the disturbances from the DC and 60 Hz power source for clearer result analysis. We used a PI controller to perform the closed loop tracking control of the motor around the yaw axis, causing the motor to perform periodic motions at 20 s with amplitude 0.05 rad and frequency 1 Hz so that the thin plate swung back and forth. From the perspective of the thin flexible plate, this motion can be considered a periodic disturbance. Figure 10 displays the tracking error and control input of the motor around the yaw axis, which produced periodic steady-state error of approximately 4%. Figure 11 lists the measurement results obtained from the piezoelectric sensors without vibration suppression. As can be seen, the periodic motions of the motor induce clear periodic vibration responses at 1 Hz in the thin plate output. FFT results (Figure 11b,c) revealed that the first mode also produced vibrations at 1.4 Hz, which is in agreement with the results obtained from finite element simulations. The peak values in the FFT plots revealed that the vibration responses in the flexible structure are influenced primarily by periodic disturbances. To suppress the vibrations in the thin plate during dynamic tracking motions, we placed a piezoelectric actuator and sensor on the thin flexible plate and reduced the amount of vibration in the structure using active vibration-suppression control.

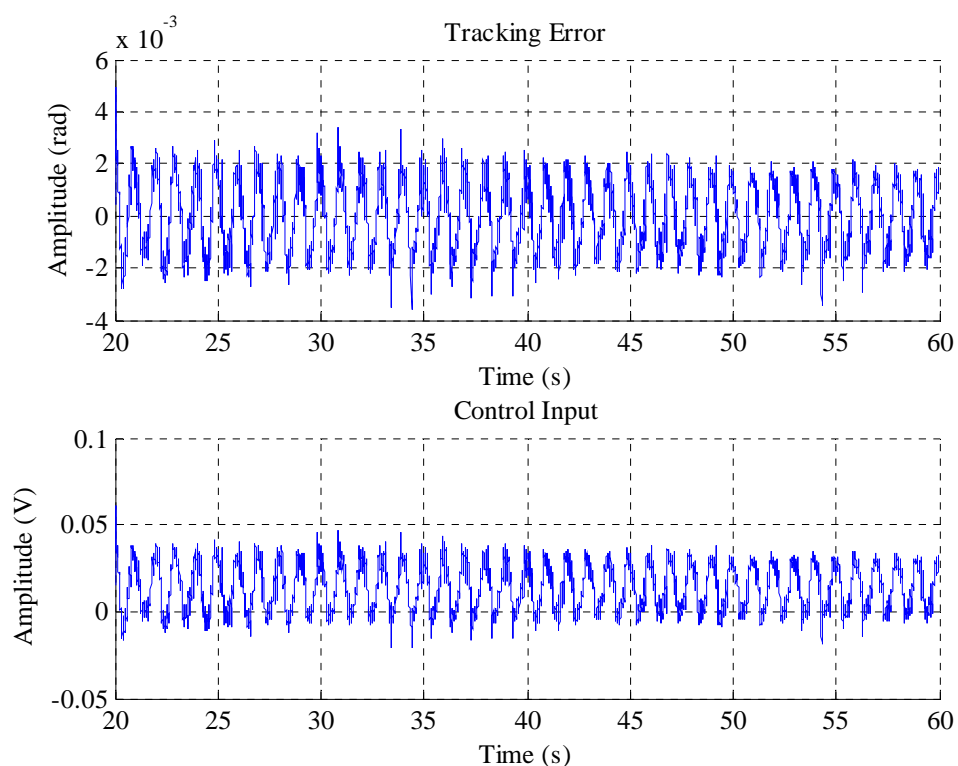


Figure 10. Periodic tracking results of the Yaw axis motor: tracking error (**top**); and control input (**bottom**).

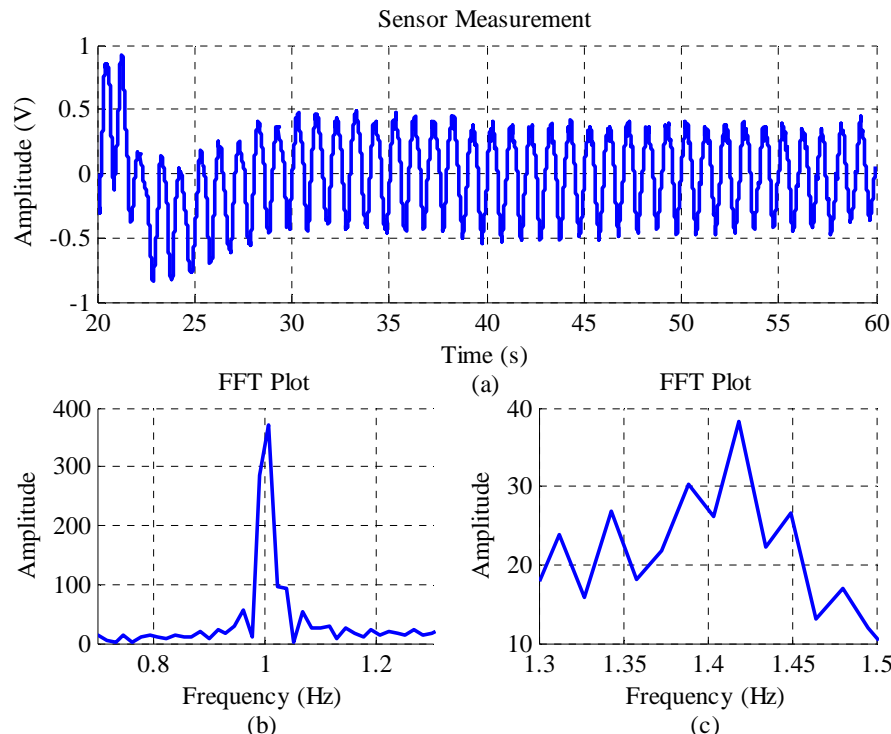


Figure 11. Flexible plate output response and FFT analysis without vibration suppression: (a) time response of uncontrolled system output, (b) FFT results at 1 Hz, and (c) FFT results at resonance frequency.

5.2. Piezoelectric Vibration Control

This study examines the active vibration suppression effects of the used three control algorithms: AFSMC, RC, and hybrid AFSMC/RC. The design parameters of the AFSMC controller were set as follows: $gu = 0.2$, $gs = 0.4$, and $\gamma_a = 0.2$. Using the time-domain system identification method, we obtained the mathematical model of the thin flexible plate system for the repetitive controller design. The relevant parameter setting was $k_r = 0.15$, and a low-pass q filter with a 10 Hz cutoff frequency was adopted to ensure the robustness of the repetitive controller. Figure 12 shows the vibration response results of the thin plate with active vibration-suppression control performed by various controllers. The AFSMC controller proved highly effective in suppressing vibrations in the thin plate; however, periodic responses remained while in steady state. RC proved more effective in reducing the periodic output in steady state; however, the initial rate of convergence was slow (40 s to reach steady state), and the amplitudes were greater. This can be attributed to an overly conservative learning gain k_r and low-pass filter q , the purpose of which was to ensure that the unmodeled dynamics in the system did not cause instability in the RC system. The hybrid AFSMC/RC control algorithm provided the benefits of AFSMC as well as RC, resulting in swift convergence (at approximately 25 s) as well as improved output responses during steady state. Figure 13 presents a comparison of the performance of the three controllers with regard to the active suppression of vibrations. The frequency band was divided into three ranges to facilitate analysis: (1) low-frequency peaks were dominated by the dynamic response of the mechanical system; (2) peak values at 1 Hz were caused by periodic excitations of the motor; and (3) peak values at 1.4 Hz were associated with the natural resonance frequency of the thin plate. AFSMC is clearly able to reduce the effects of disturbances at low frequencies and largely eliminate disturbances at 1 Hz resulting from the periodic motions of the motor. RC proved effective in suppressing vibration responses at 1 Hz; however, it was shown to amplify responses at lower frequencies as well as at natural resonance frequency of the thin plate. The hybrid AFSMC/RC control was shown to reduce output responses in all three frequency ranges.

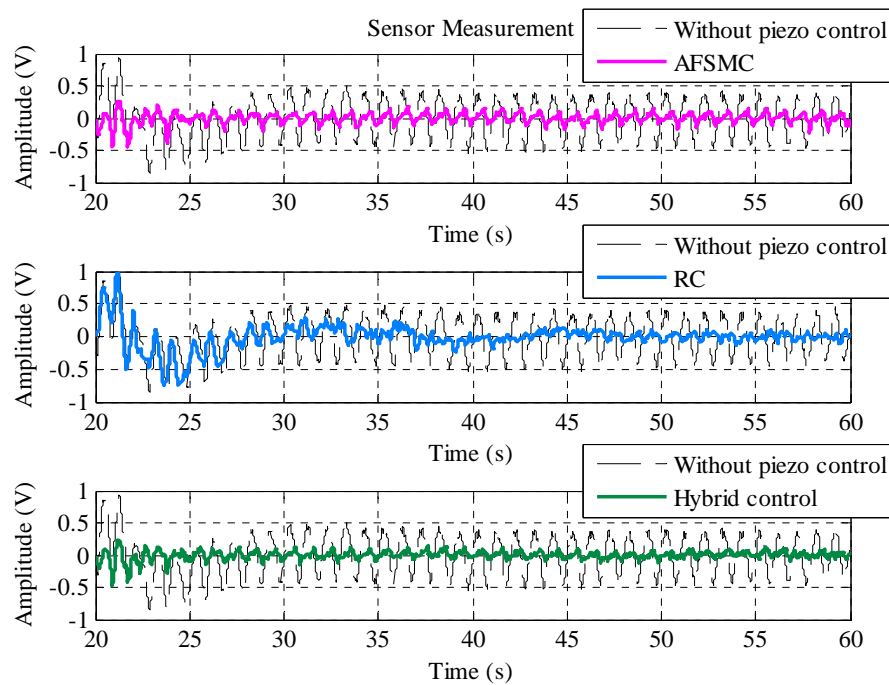


Figure 12. Piezoelectric vibration control in flexible structure: Controlled output responses obtained using: (top) AFSMC; (middle) RC; and (bottom) hybrid AFSMC/RC method.

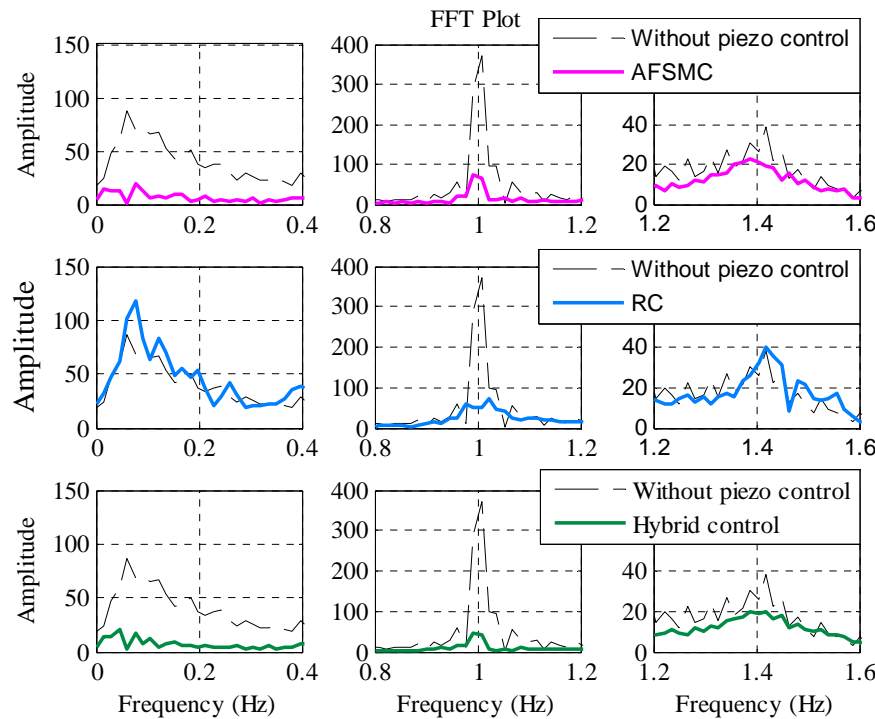


Figure 13. Piezoelectric vibration control for the flexible structure system: FFT analysis (left) low frequency range; (middle) 1 Hz; and (right) resonance frequency of 1.4 Hz.

Figure 14 shows the control input for each type of control. As can be seen, the control input of AFSMC shows continuous fluctuations. This is because the rule bank changes with each sampling point, and the continuous switching back and forth produces this chattering. The RC maintains periodic control input after the output converges to cope with the continuous excitation. As for the

control input of the hybrid control, the graph shows overlapping effects of the swift rule bank switching in AFSMC and the learning process in RC, which also presents greater control efforts. Figures 15 and 16, respectively, present the variations in the rule banks of AFSMC and hybrid control. The resulting variations in the two rule banks are similar; i.e., they both converge to within a stable range because they use the same AFSMC design parameters. When using the hybrid control, rules C3, C4, and C5 resulted in smaller fluctuations. This is because the addition of RC reduces the periodic errors, thereby enabling the rule bank to achieve the control objective without many dramatic changes.

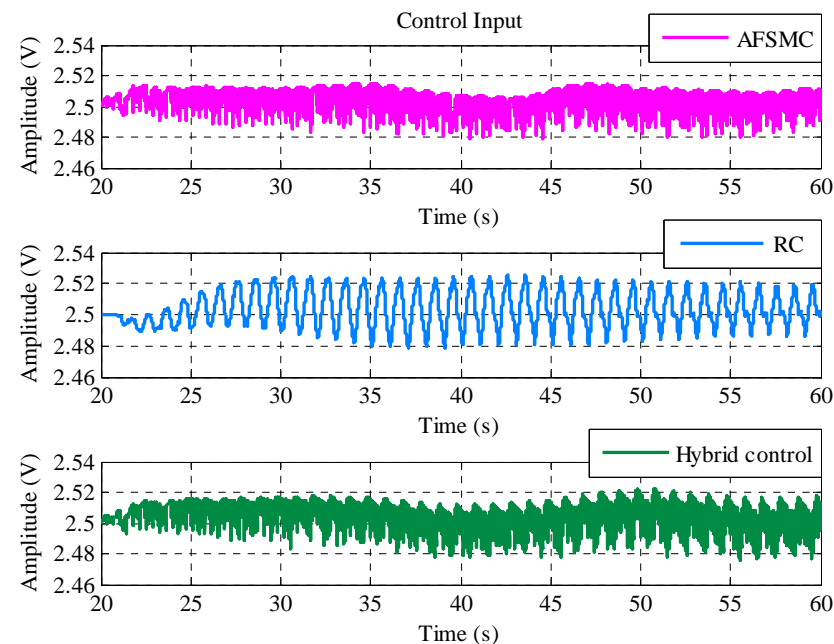


Figure 14. Piezoelectric vibration control for the flexible structure system: control input.

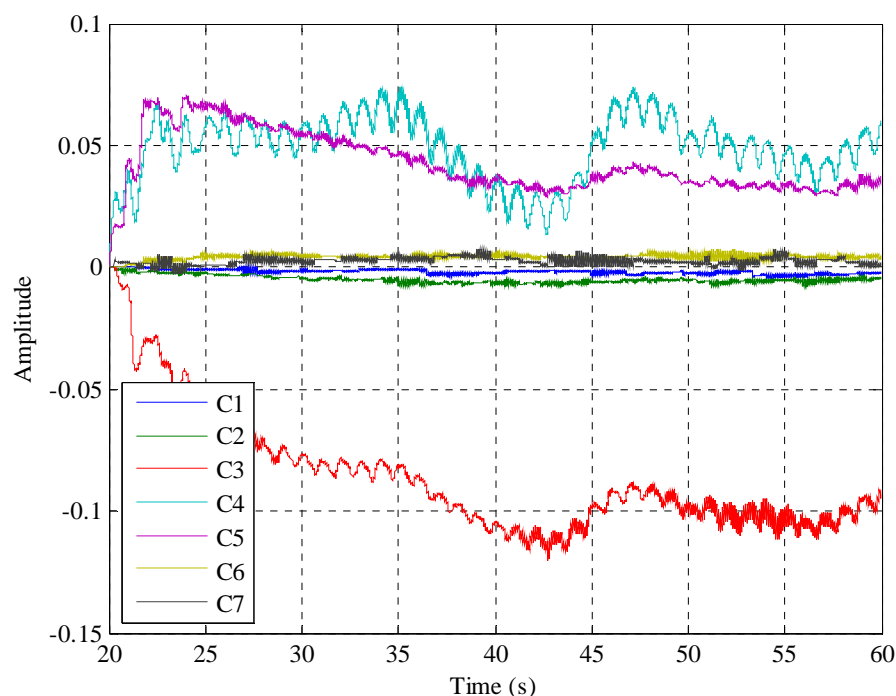


Figure 15. Fuzzy rule bank used in AFMSC vibration control system.

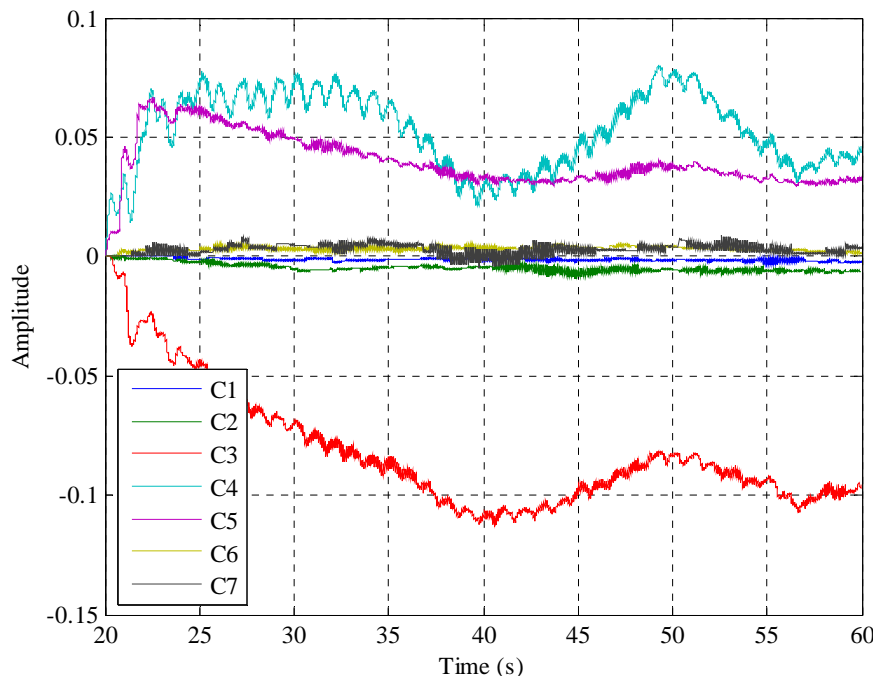


Figure 16. Fuzzy rule bank used in hybrid AFSMC/RC vibration control system.

6. Conclusions

This paper presents a novel approach to the active suppression of complex vibration responses in large flexible structures undergoing rotary motions. We applied piezoelectric materials to a thin flexible plate and then excited the plate by performing periodic motions in the motor system. The piezoelectric vibration control system was then examined using AFSMC, RC, and hybrid AFSMC/RC control algorithms. Experimental results show that AFSMC or RC can be used alone to attenuate periodic disturbances; however, the AFSMC controller was shown to reduce vibrations over a wider range of frequencies. Combining the AFSMC and RC controllers resulted in superior vibration suppression effects.

Acknowledgments: The authors would like to thank Ministry of Science and Technology, Taiwan, for providing financial support of this research under grant number MOST-101-2221-E-011-007. They are also thankful to Yu-Hsi Huang for valuable discussions and comments on this study.

Author Contributions: Chi-Ying Lin conceived and designed the active vibration control system, analyzed the results, and wrote the paper. Hong-Wu Jheng performed the vibration suppression control experiments and the data collection.

Conflicts of Interest: The authors declare no conflict of interest.

References

- Iorga, L.; Baruh, H.; Ursu, I. A review of H_∞ robust control of piezoelectric smart structures. *Appl. Mech. Rev.* **2008**, *61*, 1–15. [[CrossRef](#)]
- Lin, J. A vibration absorber of smart structures using adaptive networks in hierarchical fuzzy control. *J. Sound Vib.* **2005**, *287*, 683–705. [[CrossRef](#)]
- Kang, Y.K.; Park, H.C.; Hwang, W.; Han, K.S. Optimum placement of piezoelectric sensor/actuator for vibration control of laminate beams. *AIAA J.* **1996**, *34*, 1921–1926. [[CrossRef](#)]
- Tso, S.K.; Yang, T.W.; Xu, W.L.; Sun, Z.Q. Vibration control for a flexible-link robot arm with deflection feedback. *Int. J. Nonlinear Mech.* **2003**, *38*, 51–62. [[CrossRef](#)]
- Shan, J.; Liu, H.T.; Sun, D. Slewing and vibration control of a single-link flexible manipulator by positive position feedback (PPF). *Mechatronics* **2005**, *15*, 487–503. [[CrossRef](#)]

6. Ahmad, M.A.; Ismail, R.R.; Ramli, M.S.; Zawawi, M.A.; Hambali, N.; Ghani, N.M.A. Vibration control of flexible joint manipulator using input shaping with PD-type fuzzy logic control. In Proceedings of the IEEE International Symposium on Industrial Electronics, Seoul, Korea, 5–8 July 2009; pp. 1184–1189.
7. Park, H.W.; Yang, H.S.; Park, Y.P.; Kim, S.H. Position and vibration control of a flexible robot manipulator using hybrid controller. *Robot. Autom. Syst.* **1999**, *28*, 31–41. [[CrossRef](#)]
8. Lin, J.; Chao, W.S. Vibration suppression control of a beam-cart system with piezoelectric transducers by decomposed parallel adaptive neuro-fuzzy control. *J. Vib. Control* **2009**, *15*, 1885–1906. [[CrossRef](#)]
9. Shin, H.C.; Choi, S.B. Position control of a two-link flexible manipulator featuring piezoelectric actuators and sensors. *Mechatronics* **2001**, *11*, 707–729. [[CrossRef](#)]
10. Moudgal, V.G.; Kwong, W.A.; Passino, K.M.; Yurkovich, S. Fuzzy learning control for a flexible-link robot. *IEEE Trans. Fuzzy Syst.* **1995**, *3*, 199–210. [[CrossRef](#)]
11. Lin, J.; Huang, C.J.; Chang, J.; Wang, S.W. Vibration suppression controller for a novel beam-cart-seesaw system. In Proceedings of the American Control Conference, Baltimore, MD, USA, 30 June–2 July 2010; pp. 1526–1531.
12. Lin, J.; Zheng, Y.B. Vibration suppression control of smart piezoelectric rotating truss structure by parallel neuro-fuzzy control with genetic algorithm tuning. *J. Sound Vib.* **2012**, *331*, 3677–3694. [[CrossRef](#)]
13. Lin, C.Y.; Chiu, W.H.; Lin, J. Rejecting multiple-period disturbances: Active vibration control of a two degree-of-freedom piezoelectric flexible structure system. *J. Vib. Control* **2015**, *21*, 3368–3382. [[CrossRef](#)]
14. Lin, C.Y.; Chang, C.M. Hybrid proportional derivative/repetitive control for active vibration control of smart piezoelectric structures. *J. Vib. Control* **2013**, *19*, 992–1003. [[CrossRef](#)]
15. Huang, S.J.; Huang, K.S. An adaptive fuzzy sliding-mode controller for servomechanism disturbance rejection. *IEEE Trans. Ind. Electron.* **2001**, *48*, 845–852. [[CrossRef](#)]
16. Huang, S.J.; Lin, W.C. Adaptive fuzzy controller with sliding surface for vehicle suspension control. *IEEE Trans. Fuzzy Syst.* **2003**, *11*, 550–559. [[CrossRef](#)]
17. Huang, S.J.; Shieh, H.W. Motion control of a nonlinear pneumatic actuating table by using self-adaptation fuzzy controller. In Proceedings of the IEEE International Conference on Industrial Technology (ICIT), Churchill, Victoria, Australia, 10–13 February 2009; pp. 1–6.
18. Narendra, K.; Annaswamy, A. A new adaptive law for robust adaptation without persistent excitation. *IEEE Trans. Autom. Control* **1987**, *32*, 134–145. [[CrossRef](#)]
19. Tomizuka, M.; Tsao, T.C.; Chew, K.K. Analysis and synthesis of discrete-time repetitive controllers. *J. Dyn. Syst. Meas. Contr.* **1989**, *111*, 353–358. [[CrossRef](#)]
20. Tomizuka, M. Zero phase error tracking algorithm for digital control. *J. Dyn. Syst. Meas. Contr.* **1987**, *109*, 65–68. [[CrossRef](#)]
21. Skogestad, S.; Postlethwaite, I. *Multivariable Feedback Control: Analysis and Design*; John Wiley & Sons: Hoboken, NJ, USA, 1996.



© 2017 by the authors. Licensee MDPI, Basel, Switzerland. This article is an open access article distributed under the terms and conditions of the Creative Commons Attribution (CC BY) license (<http://creativecommons.org/licenses/by/4.0/>).